Balanced JAK/STAT signaling is critical to maintain the functional and structural integrity of the *Drosophila* respiratory epithelium

Xiao Niu[1], Christine Fink[1], Kimberley Kallsen[2,4], Viktoria Mincheva[1], Sören Franzenburg[3], Ruben Prange[1], Judith Bossen[1], Holger Heine[2, 5], Thomas Roeder[1, 5]

[1]Kiel University, Zoology, Dept. of Molecular Physiology, Kiel, Germany

[2]Research Center Borstel, Dept. of Innate Immunity, Borstel, Germany

[3]Kiel University, IKMB, Kiel, Germany

[4]Current address: Boehringer Ingelheim, Ingelheim, Germany

[5]German Center for Lung Research, Airway Research Center North, Kiel, Germany

Summary

Signals mediated by the Janus kinase (JAK)/signal transducer and activator of transcription (STAT) pathway play a central role in maintaining homeostasis in a multitude of tissues. A large number of studies have shown that this role is particularly prominent in the lungs. Deregulation of the JAK/STAT signaling pathway is causally linked with various, mostly chronic, lung diseases, including lung cancer, asthma, and chronic obstructive pulmonary disease. To elucidate the molecular framework that explains how deregulated JAK/STAT signaling gives rise to pathogenic states, we used the fruit fly *Drosophila* as a model. While the JAK/STAT pathway is characterized by high structural diversity and complexity in vertebrates, it is relatively simple in *Drosophila*. The JAK/STAT pathway was active in almost all respiratory epithelial cells of larvae and adult flies. Stressful stimuli, such as cigarette smoke, evoked strong and regionalized activation of the JAK/STAT pathway, which was most likely driven by the concurrently induced ligand Unpaired 2. Inhibition of JAK/STAT signaling induced apoptotic processes in epithelial cells. The aforementioned chronic lung diseases are associated with increased activity of the JAK/STAT pathway and are treated with specific JAK inhibitors. Therefore, we investigated the effects of increased JAK/STAT signaling in the respiratory epithelium of *Drosophila*. Ectopic activation of the JAK/STAT pathway led to premature death at the larval or pupal stage. Furthermore, it induced major structural changes in epithelial cells, which almost completely lost their typical characteristics. These structural changes led to considerable thickening of the

epithelium, substantial narrowing of the air-conducting space, and disruption of the tracheal epicuticular structure. Pharmacological interference of JAK/STAT signaling reverted this phenotype. Activation of the JAK/STAT pathway also affected vesicle-mediated transport, which led to erroneous trafficking of typical junction proteins. In summary, these results demonstrate that balanced JAK/STAT signaling is essential for the normal functionality of the respiratory epithelium and thus the entire organ. A basal level of JAK/STAT signaling is required for cellular processes such as growth and division. However, chronic overactivation of this signaling leads to massive structural changes that are closely related to pathologies typically seen in chronic inflammatory lung diseases.

Introduction

The Janus kinase (JAK)/signal transducer and activator of transcription (STAT) signaling system is of central importance for several critical physiological processes including development, tissue homeostasis, and immune responses [1]. Various cytokines, growth factors, and related signaling compounds signal via this evolutionarily conserved system [2]. The JAK/STAT signaling pathway effectively transduces external signals into desired cellular responses despite having relatively few essential components. Signaling via this pathway is therefore straightforward and allows environmental factors to directly influence transcriptional activity in cells, thereby linking important biological processes with environmental cues [3]. Moreover, JAK/STAT signaling is tightly associated with a great variety of immune responses. JAK/STAT signaling acts downstream of a plethora of cytokines that transmit immune-related information and is, therefore, a central hub in various immunocompetent cells [4-7]. Deregulation of this signaling pathway is directly linked with numerous human diseases, including cancer and inflammatory diseases [5, 8, 9].

Lung diseases are often associated with deregulated JAK/STAT signaling. Such deregulation can arise due to mutations and polymorphisms in genes associated with JAK/STAT signaling. In addition, this signaling is activated by stressors, infections, and injuries. This might cause sustained chronic inflammation of the airways and/or alveoli, which is closely associated with the onset and chronification of various lung diseases.

Chronic obstructive pulmonary disease (COPD), asthma, idiopathic pulmonary fibrosis, and lung cancer are causally associated with deregulated JAK/STAT signaling [10]. This signaling is not only of great importance during organ development, but also plays a central role in maintaining tissue and immune homeostasis, especially in response to stressors, infection, and damage [11, 12]. Functional JAK/STAT signaling is required to cope with stressful stimuli such as hyperoxia in the airway epithelium [10]. Deregulation of this signaling in the airways is associated with pathological states. Specifically, chronically reduced JAK/STAT signaling is associated with impaired repair capacities [11], while increased JAK/STAT signaling leads to cell proliferation that can cause cancer [13]. Despite its simple general organization, the JAK/STAT signaling pathway is characterized by multiple redundancies in vertebrates. A multitude of elements function at each level of the JAK/STAT signaling pathway; for example, more than 50 cytokines can activate this pathway [6]. Moreover, deregulation of JAK/STAT signaling in different motile and resident cell types found in the lungs is associated with chronic lung diseases. Therefore, models with a much simpler JAK/STAT pathway and a less complicated cellular composition in the airways should help to elucidate the effects of dysfunctional JAK/STAT signaling, especially in airway epithelial cells.

Simple models such as the fruit fly *Drosophila melanogaster* are thus a reasonable alternative to analyze the relevance of JAK/STAT signaling in the airways. While this signaling pathway exhibits broad diversification at all levels in mammals, it involves a

single receptor (Domeless), one JAK (Hopscotch), and one STAT transcription factor (Stat92E) in *Drosophila* [2, 14]. This low level of redundancy offers a unique advantage to investigate the JAK/STAT pathway in tissues of interest. JAK/STAT signaling is highly important for many processes, including development, in flies. The tracheal system does not form when JAK/STAT signaling is abolished in tracheal primordia [15, 16]. Unpaired (Upd), a major ligand of this pathway, is expressed in tracheal pits and initiates JAK/STAT signaling in this organ primordium [17]. A lack of JAK/STAT signaling during very early phases of tracheal development leads to a lack of expression of developmentally relevant genes such as trachealess (*trh*), which is essential to instruct important phases of tracheal development including cell movement and elongation, as well as invagination processes that lead to tube formation [15, 18]. This is consistent with the important role of JAK/STAT signaling during lung development in vertebrates [19, 20].

The current study aimed to determine the physiological significance of JAK/STAT signaling in a simple, but fully functional, airway system. Therefore, we studied the larval airway system of the fruit fly *D. melanogaster* and evaluated if the JAK/STAT signaling pathway is active in functional airway epithelial cells and if stress signals modify the activity of this pathway. Furthermore, we investigated if deregulation of this pathway leads to disease-associated phenotypes in this simple airway system.

Results

The JAK/STAT pathway is strongly activated in the trachea during embryogenesis and is important for organ development [21]. However, the exact pattern of its activation is unclear. In this study, we used the *Stat92E-GFP* reporter [21] to monitor activation of the JAK/STAT pathway concurrently with *btl>LacZ.nls* [22], which specifically labels the trachea. Figure 1A schematically depicts the JAK/STAT pathway in *Drosophila*. Activation of the *Stat92E* was enhanced in a central region in the trachea, mainly in the transverse connective area (Fig. 1B–D). To confirm the importance of the JAK/STAT pathway in the development of the *Drosophila* respiratory system, we manipulated its activity in the trachea by driving expression of a dominant-negative isoform of Domeless (*Dome.DN*) using *btl-Gal4*. Although some animals grew to the larval stage, all died before reaching the pupal stage (Fig. 1E). Microscopic analysis of surviving larvae showed that the dorsal trunk (DT) was absent (Fig. 1E''). Time-lapse imaging of trachea-specific *Dome.DN* expression in embryos revealed that all tracheal segments were fused at stage 15; however, the DT subsequently separated (Fig. 1F and H). Next, we tested the effects of ectopic activation of the JAK/STAT pathway induced by expression of the ligand (Upd3) or the constitutively active JAK-allele (Hop.CA) on tracheal development. These animals died prematurely at the embryo or larval stage (Fig. 1E). Microscopic analysis of larvae and embryos showed that the tracheal segment separated at the larval stage (Fig. 1E'''–E''''); however, the disconnection of segments was due to failure of their fusion at the beginning of tracheal development (Fig. 1G and H). In contrast with animals that expressed *upd3*,

most *Hop.CA*-expressing animals exhibited a full tracheal tree. However, they all died at the first larval stage, which indicates that JAK/STAT signaling influences tracheal development after the first tracheal structures have formed.

To determine if the JAK/STAT pathway also operates in functional airway epithelium, namely, the larval tracheal system, we used the STAT reporter line mentioned above. STAT signaling was active in all regions of the tracheal system in third instar larvae (Fig. 2A). JAK/STAT activity was reduced in the posterior zone of the trachea, tenth tracheal metamere (Tr10), where cells progressively undergo apoptosis in response to trachea metamorphosis (Fig. 2B). However, JAK/STAT activity was much stronger in regions such as Tr2, spiracular branch (SB) and dorsal branch (DB), where cells re-enter the cell cycle at this developmental stage than in nearby areas containing quiescent cells (Fig. 2C and D). We next evaluated if JAK/STAT activity is observed in airway epithelial cells of adults. The same approach detected substantial reporter activity in airway epithelial cells of fully developed adults (Fig. 2E and E'). Inhibition of JAK/STAT signaling changed the fate and morphology of larval airway epithelial cells (Fig. 2F). This inhibition was achieved by ectopically expressing *Dome.DN*. These cells gradually lost their typical shape, and apoptotic processes were initiated 2 days after induction of ectopic expression. This induction of apoptosis was confirmed by detection of Dcp1 in cells with typical apoptotic features (Fig. 2G and H). Apoptosis was induced to an even greater extent (and faster) in stem cells of the larval tracheal system, where Dcp1-positive cells were observed on 1 day

after induction of ectopic *Dome.DN* expression (Fig. 2I–K). The JAK/STAT pathway was activated throughout the entire tracheal system. Therefore, we evaluated expression of the three Upd ligands in this system. Experiments using the corresponding enhancer-*Gal4* lines demonstrated that *upd2* was highly expressed in the tracheal system (Fig. S1).

To elucidate the effects of JAK/STAT deregulation in the tracheal system initiated at different time points during larval development, we employed the temperature-inducible Gal4/Gal80[ts] system (Fig. 3A). We first tested the effects of inhibition of the tracheal JAK/STAT pathway induced by ectopic expression of *Dome.DN* on survival and larval structure (Fig. 3B). Ectopic expression was initiated at three time points during larval development (Fig. 3B). Larval mortality was higher, the earlier expression was initiated. No larvae survived to the pupal stage (Fig. 3C). On the other hand, activation of JAK/STAT signaling induced by ectopic expression of *upd3* or *Hop.CA* led to lower levels of larval death. In both cases, no pupae developed into adults. Furthermore, we analyzed the effects of this intervention on tracheal structure. Whereas *Dome.DN* overexpression elicited only minor effects on tracheal structure, *upd3* or *Hop.CA* overexpression caused substantial epithelial thickening (Fig. 3D–H). Quantitative evaluation revealed that ectopic overexpression of *Hop.CA* greatly increased epithelial thickness (Fig. 3H). Experiments involving mosaic expression of *Hop.CA* driven by *vvl-FLP*, *CoinFLP-Gal4, UAS-EGFP (vvl-coin)* demonstrated that this effect was cell-autonomous. Cells that expressed *Hop.CA* were much thicker than neighboring cells that did not (Fig. 3I). Treatment with various JAK

inhibitors [23] reversed epithelial thickening induced by ectopic overexpression of *Hop.CA* in the trachea (Fig. 3J–L). Treatment with Baricitinib, Oclacitinib, or Filgotinib reduced epithelial thickening by more than 60% (Fig. 3L).

To elucidate the mechanisms underlying this structural response, we analyzed the phenotype in more detail. The length of a defined area of the tracheal system (between Tr8 and Tr9), the length-thickness product, and the cell number were quantified (Fig. 4A and B). Length was unaffected by manipulation of JAK/STAT signaling in the trachea, with the exception that it was reduced after 4 days of ectopic *Dome.DN* expression (Fig. 4B). Consequently, the length-thickness product mirrored the findings made when assessing thickness. However, the number of cells in the Tr8-Tr9 region of the trachea with manipulated JAK/STAT signaling was similar to that in matching controls (Fig. 4B''). Hence, the thickening was due to an increase in cell volume, not an increase in cell number. To determine if this thickening is an artifact caused by the isolation method, we directly fixed the trachea in situ or isolated it in cell culture medium with the same osmolarity as hemolymph. The same thickening was observed in both cases (Supplemental Fig. 2). To quantify the time course of this thickening, we subjected the trachea to different treatment regimens prior to analysis. At least 2 days of ectopic expression were necessary to induce this phenotype (Fig. 4C–E).

After demonstrating that JAK/STAT signaling operates in a fully functional tracheal system and that deregulation of its activation substantially impacts the structure of the airway

system, we aimed to identify conditions under which JAK/STAT signaling activity is increased. To this end, we subjected flies to two stressful conditions that are related to the airway system, namely, cigarette smoke exposure and hypoxia. Whereas hypoxia did not affect the activities of the JAK/STAT pathway reporter or the corresponding ligands (Upd2 (Fig. 5D–F) and Upd3 (Fig. 5J–L)), smoke exposure induced expression of both *upd2* and *upd3* as well as activation of the JAK/STAT pathway reporter (Fig. 5A–C, F–I, and L). Induced expression was mostly confined to a highly sensitive region close to the spiracles (Tr9 and Tr10) (Fig. 5B, F, H, and L).

To investigate the molecular mechanisms underlying the effects of chronic JAK/STAT activation on the airways, we performed RNA-sequencing analysis of tracheal cells expressing *Hop.CA* in third instar larvae. The validity of this experimental procedure was supported by the induced expression of *hopscotch* (including *Hop.CA*) and *Socs36E* (one of the best-characterized Stat92E target genes) [21], which were upregulated 35-fold and 2.7-fold, respectively ($p < 10^{-12}$). Principal component analysis of biological replicates separated control and overexpression samples into different groups (Fig. 6A, middle). Finally, the expression of 2004 genes was statistically significantly regulated, with 1128 downregulated genes and 876 upregulated genes ($p < 0.05$). A circular heatmap of 707 differentially expressed genes ($p < 0.01$ and fold change > 2) is presented (Fig. 6A). Moreover, we analyzed changes in expression upon ectopic silencing of the JAK/STAT pathway using *Dome.DN*. A Venn diagram revealed that there was a statistically significant

overlap in the cohorts of genes regulated by both interventions (Fisher's exact test, $p < 0.0001$; Fig. 6B).

To further elucidate the molecular mechanisms functioning in the thickened epithelium, we performed promotor scan studies and Gene Ontology (GO) analyses. Genes with the highest rates of induction supported by the lowest p-values were subjected to promoter scanning (Pscan) analysis. Putative genes directly regulated by the JAK/STAT pathway were identified (Tables 1 and 2). Among these highly regulated genes, the largest group contained genes that encoded products involved in innate immunity, including seven antimicrobial peptide genes (*IM1, IM2, IM4, IM14, CG5791, CG5778,* and *Drs*). All these antimicrobial peptides, except for Drs, contain one or two CXXC regions. These CXXC-containing peptides belong to the family of Bomanins, whose expression is highly induced following bacterial or fungal infection, and high levels of the corresponding mature peptides are found in the hemolymph of infected flies [24].

Next, we analyzed all significantly regulated genes based on KEGG and GO annotations. Six terms in KEGG pathway analysis and nine categories in GO analysis were enriched among these genes according to their predicted functions (Table S1 and Fig. 7).

One striking feature of the epithelium with chronically activated JAK/STAT signaling was induced expression of genes involved in vesicle-mediated transport (Fig. 7). GO analysis demonstrated that this term was enriched among 32 regulated genes that had been assigned to vesicle-mediated transport. All these genes were upregulated, except for one

(CG5946). However, according to a Pscan analysis, these genes did not seem to be direct JAK/STAT targets since a Stat92E promoter binding was not enriched (table S2 and S3). The transcript levels of genes related to epicuticle development were reduced. Fifty-five genes relevant to cuticle development were regulated, of which 40 were downregulated. In addition, other biological processes such as muscle cell differentiation, cellular protein-containing complex assembly, RNA processing, translation, and detection of chemical stimuli were significantly enriched. In the latter three categories, the number of upregulated genes was similar to the number of downregulated genes. A schematic representation of the different biological processes superimposed on a scheme of an epithelial cell is shown (Fig. 7B). One interesting result was that endocytosis and vesicle-mediated transport were impaired. To analyze this further, we focused on two peripheral membrane-binding proteins, namely, Coracle (Cora), a component of septate junctions and Armadillo (Arm), a component of adherens junctions. Both proteins depend on vesicle transport to reach their destinations [25, 26] (Fig. 8A). Immunofluorescence analysis of *Hop.CA*-overexpressing animals revealed that Arm and Cora accumulated in the cytoplasm, which is indicative of dysfunctional endosomal transport (Fig. 8B–E). We also observed a stenosis phenotype with tube narrowing. This arose when epithelial cells expressed *Hop.CA* at very high levels, as indicated by strong green fluorescence (Fig. 8F and G and Fig. S2). The lumen narrowing observed here is reminiscent of the phenotype caused by

246 mutations of the coatomer protein complex (COP)I or COPII complexes, which are
247 required for the efficient secretion of proteins that drive tube expansion [27, 28] (Fig. 8H).
248 Cuticle development was identified as another regulated biological process based on
249 transcriptome data. This process is dependent on secretion in the larval trachea, and
250 chitin-rich structures, called taenidia, are believed to make tubes flexible as well as
251 sufficiently strong in order to avoid collapse [29]. The chitin structure in the trachea was
252 unsorted in *Hop.CA*-expressing animals compared with control tubes (Fig. 9A and B).
253 Chitin staining revealed that the highly organized structure of the chitinous intima was
254 almost completely lost in *Hop.CA*-expressing animals (Fig. 9C). Mosaic analysis
255 demonstrated that the trachea was structurally disorganized where *Hop.CA* was expressed
256 (Fig. 9D–F).
257 The effects of activating the JAK/STAT pathway on the epithelium were time-dependent.
258 To determine if a weaker expression of *Hop.CA* induces similar phenotypes, we used
259 another trachea-specific Gal4-driver, namely, PPK4 (also called *nach-Gal4*). In the *nach-*
260 *Gal4* line, *Gal4* is expressed from the late embryo stage, is strongly expressed in the early
261 L1 and late L2 stages, at which point expression is stronger than that driven by *btl-Gal4*,
262 but is weakly expressed at other larval stages [30, 31]. Microscopy analysis of the trachea
263 showed that weak expression of *Hop.CA* in the trachea promoted epithelial thickening (Fig.
264 10A and B). However, epithelial thickening after 4 days of *Hop.CA* induction was slightly
265 lower in *nach>Hop.CA* than in *btl>Hop.CA* (Fig. 10D). On the other hand, weakly driven

upd3 expression in the trachea resulted in identical changes as those observed using *btl-Gal4* (Fig. 10C and E). Finally, we used the same driver to inhibit JAK/STAT signaling in the trachea by expressing *Dome.DN*. Animals died prematurely at the larval stage and their tracheas were filled with liquid, demonstrating that functionality was impaired (Fig. 10F).

Discussion

The present study aimed to elucidate the significance of the JAK/STAT signaling pathway in the respiratory epithelium. We used the fruit fly *D. melanogaster* owing to the experimental advantages of this system and the unique simplicity of the JAK/STAT signaling pathway. JAK/STAT signaling exhibited tonic activity in almost all respiratory epithelial cells and its activity was substantially enhanced by exposure to cigarette smoke. Stress-induced induction of the JAK/STAT signaling pathway and the corresponding cytokines is also observed in primary human respiratory epithelial cells, suggesting that the activation and mechanism-of-action of JAK/STAT signaling are similar in human and *Drosophila* respiratory epithelial cells [32]. Our finding that the JAK/STAT signaling pathway operated in airway epithelial cells of embryos, larvae, and adults implies that it plays a central role in these cells at all developmental stages. The JAK/STAT pathway was previously reported to be important for embryonic development of the tracheal system [33]. We clarified the sequence of developmental steps in which this signaling pathway plays a central role. The JAK/STAT signaling pathway is particularly important for

development and maintenance of the DT. Tracheal JAK/STAT signaling is required during development of the adult tracheal system at the pupal stage [34]. This is consistent with our finding that the various interventions induced lethality in the pupal stage at the latest. It is a matter of debate whether JAK/STAT signaling is essential for mammalian lung development. However, the prevailing view that JAK/STAT signaling is not essential for embryonic lung development [11] has been challenged by recent studies [20]. Although JAK/STAT signaling is essential for different aspects of tracheal development, the major focus of the current study was on the role of this signaling in maintaining homeostasis in the fully functional airway epithelium. Therefore, we chose *Drosophila* larvae as a model because they possess fully functional airways that must perform gas exchange for survival and growth of the animal. Respiratory epithelial cells in larvae are terminally differentiated and cannot divide, but increase in size as larvae grow. We demonstrated that the JAK/STAT signaling pathway was essential in the larval airway epithelium and that its blockade induced apoptosis. This implies that the JAK/STAT pathway plays a central role in homeostatic processes in this organ, which also appears to be the case in mammalian airway epithelia. Perturbation of JAK/STAT signaling induces apoptosis in cell lines derived from airway epithelia [35], and this seems to be particularly relevant for growing tissues and cells that can still divide or grow [36]. This ability to grow might be one reason for the high susceptibility of *Drosophila* airway epithelial cells to blockade of JAK/STAT signaling. Thus, cytokines that activate the JAK/STAT signaling pathway act as survival factors at least

306 in part, especially where repair mechanisms are operative. Functional JAK/STAT signaling
307 is also required for regenerative processes after epithelial damage [11, 12], the response
308 to infections [37], and the reaction to hyperoxia [38]. This indicates that JAK/STAT signaling
309 in mammalian airway epithelial cells and the *Drosophila* trachea is particularly relevant
310 for a protective reaction to stressful stimuli. Consistently, we demonstrated that JAK/STAT
311 signaling was normally active in airway epithelial cells of *Drosophila* larvae. A basal level
312 of JAK/STAT signaling was observed in these cells and this signaling was further activated
313 in response to very strong stressors such as chronic exposure to smoke particles. There
314 appears to be an organ-autonomous JAK/STAT signaling system, with expression and
315 release of the cytokines Upd2 and Upd3, and activation of a JAK/STAT-dependent response
316 induced in the same regions of the tracheal system. A comparable, stress-induced system
317 has been identified in the intestinal epithelium of flies, where highly stressful insults
318 targeting absorptive enterocytes induce production and release of the cytokine Upd3 [39,
319 40]. In contrast with the intestines, where cytokines produced by stressed enterocytes
320 induce proliferation of stem cells to replenish the enterocyte pool, the typical structure of
321 epithelial cells in the tracheal system is altered without activation of stem cells.
322 Although a threshold level of JAK/STAT signaling is required for the functionality and
323 survival of airway epithelial cells, excessive activation of this signaling is associated with
324 several lung diseases including lung cancer, acute lung injury, asthma, pulmonary fibrosis,
325 and COPD [13, 41-45]. This implies that different facets of this highly complex signaling

pathway are critically involved in the development of the majority of chronic lung diseases. Thus, maintaining homeostasis in the airway epithelium, especially with respect to its potential damage and repair, is essential for a healthy life. In this context, the JAK/STAT pathway seems to play a decisive role [11]. To study the imbalance of JAK/STAT signaling that is causally associated with the majority of chronic lung diseases and is responsible for the structural changes typically seen in these diseases, we ectopically activated JAK/STAT signaling specifically in the airway epithelium of *Drosophila* larvae. This activation induced major structural changes in the airway epithelium, mainly to the architecture of tracheal cells. Mosaic analysis demonstrated that this effect was cell-autonomous. These major structural changes of the trachea are reminiscent of those observed in asthma, COPD, acute lung injury, and lung cancer. Structural changes that permit to fulfill the original function of epithelial cells are often observed during the epithelial-to-mesenchymal transition. JAK/STAT signaling is essential for the epithelial-to-mesenchymal transition intrinsic to lung cancer [46].

Ectopic JAK/STAT pathway activation induced complex alterations to the transcriptome in airway epithelial cells. These changes affected immune-relevant genes such as those encoding antimicrobial peptides, mainly from the Bomanin family. JAK/STAT signaling typically regulates antimicrobial responses in the human airway epithelium [41]. However, chronically activated JAK/STAT signaling perturbed secretory processes and the formation of extracellular structures. The extracellular matrix defects caused by *Hop.CA*

346 overexpression are reminiscent of the pathophysiology of the aforementioned chronic
347 lung diseases that involve responses to acute or chronic injury [47]. Therefore, attempts
348 to enhance the repair capacities of epithelial cells by inducing structural changes via
349 excessive JAK/STAT signaling would also perturb normal cellular functions, such as the
350 transport of junction proteins to the membrane. This would lead to reduced barrier
351 function of the epithelium, which is a hallmark of chronic lung diseases such as asthma
352 and COPD [48-50]. We also observed epicuticular changes, which considerably influenced
353 the structure of the whole organ. However, it is difficult to identify an equivalent change
354 in vertebrates.
355 The JAK/STAT pathway is an excellent target for therapeutic intervention in many lung
356 diseases, including asthma, COPD, acute lung injury, idiopathic pulmonary fibrosis, and
357 lung cancer [43, 51-55]. We demonstrated that pharmacological interference of the
358 JAK/STAT signaling pathway reverted the structural phenotype observed upon ectopic
359 activation of this signaling and consequently flies survived. This shows that the *Drosophila*
360 model is not only suitable to study the structural effects of excessive JAK/STAT signaling
361 and the underlying molecular mechanisms, but also to screen compounds and thereby
362 identify novel therapeutic strategies.
363 It must be remembered that the vertebrate lung and insect trachea are not homologous.
364 Nevertheless, they share a high degree of similarity in terms of their development,
365 physiology, innate immunity, and operative signaling systems [56, 57]. Therefore, the fruit

366 fly is a very valuable tool to study genes associated with a great variety of chronic lung
367 diseases including asthma, COPD, and lung cancer [58-63]. This simple model can be used
368 as part of an experimental toolbox to elucidate the role of JAK/STAT signaling in the
369 airways and the effects of chronic deregulation of this signaling. In addition, it provides a
370 readily accessible experimental system that is amenable to pharmacologic interventions,
371 and allows hypotheses and intervention strategies to be easily tested.
372

373 ## Material and Methods

374 ### *Drosophila* strains and husbandry

375 *Stat92E-GFP* was used to monitor the activation of the pathway [21]; the Gal4-UAS system
376 [64] was used to target ectopic expression to the tracheal system. Gal4 drivers used were:
377 *btl-Gal4, UAS-GFP* on the 3rd chromosome, and *btl-Gal4, UAS-GFP* on the 2nd
378 chromosome (obtained from the Leptin group, Heidelberg, Germany); *upd2-Gal4*; *upd3-*
379 *Gal4* [60]; *nach-Gal4* [30]. The UAS responders included: *UAS-LacZ.nls* (BDSC 3956), *UAS-*
380 *domeΔcyt2.1* (*UAS-Dome.DN*) and *UAS-Hop.CA* (*UAS-hopTumL*) were obtained from N.
381 Perrimon [15, 65]. The *UAS-upd3* was constructed in our lab. *TubP-Gal80[ts]* (BDSC 7018)
382 were obtained from the Bloomington stock center. Unless otherwise stated, the flies were
383 raised on standard medium at 25 °C with 50–60% relative humidity under a 12:12 h
384 light/dark cycle as described earlier [66].
385

Coin-FLP expression system

Vvl-FLP/CyO; btl-moe.mRFP (BDSC 64233), *tubP-Gal80[ts]* and *CoinFLP-Gal4, UAS-2xEGFP* (BDSC 58751) were used to construct animals for the tracheal mosaic analysis. Ventral veins lacking (*vvl*) was expressed in larval tracheal clones that covered approximately 30 to 80% of the trachea [67, 68]. The genotype of the flies was *vvl-FLP*, *CoinFLP-Gal4*, *UAS-2xEGFP*/*CyO* (*vvl-coin*) and *vvl-FLP*, *CoinFLP-Gal4*, *UAS-2xEGFP*/*CyO*; *tub-Gal80[ts]* (*vvl-coin.ts*).

Developmental Viability

For developmental viability of eggs, the eggs were collected overnight and were not physically handled in any way. The number of the hatched eggs and the pupae were counted starting from two days after the collection. Each group has 4 replicates that included more than 20 eggs. For developmental viability of larvae, *tub-Gal80[ts]* was used to limit UAS responder expression at the larvae stage. Animals were raised at 18 °C to keep the UAS responder gene silent. Larvae at different instar stages were transferred to new medium at 29 °C. In this study, usually 4 replicates were performed with 30 larvae. The stage of larvae was determined via the appearance of anterior spiracles.

Determination of epithelial thickness

The trachea of L2 and L3 Larvae were carefully dissected out from the posterior side of the body in PBS. The isolated trachea was immersed in 50% glycerol and digital images captured within 15 min. L2 Larvae were distinguished from L3 larvae by the appearance

of anterior spiracles. The relative ages of L3 larvae were inferred from the size of the animal. 30 larvae were used in each group and specimens were analysed by Image J.

Drug application and determination of epithelial thickness

JAK inhibitors (Baricitinib #16707 , Oclacitinib #18722, Filgotinib #17669 - Cayman Chemicals, Michigan, USA) were diluted in DMSO [100 mM]. For later application the inhibitors were diluted 1:10 in 100% EtOH. We used 20 µl of each diluted inhibitor for 2 ml of concentrated medium (5% yeast extract, 5% corn flour, 5% sucrose, 1% low-melt agarose, 1 ml of 10% propionic acid and 3 ml of 10% Nipagin). The eggs of each crossing have been applicated on the modified medium and kept at 20 °C until the larvae reach the L2 stage. Afterwards they were incubated at 30 °C for 2 days to induce the *btl-Gal4, UAS-GFP; tub-Gal80[ts] (btl.ts*) –driver. The trachea of L3 Larvae were carefully dissected out from the posterior side of the body in the PBS. Isolated trachea was immersed in 50% glycerol and digital images captured in 15 min. 10 larvae were used for each group.

Time-lapse microscopy

All images were acquired using a ZEISS Axio Image Z1 fluorescent microscope. Embryos were dechlorinated in 3% sodium hypochlorite and immersed in Halocarbon oil 700 (Sigma Aldrich, 9002-83-9). Then the embryos were imaged after stage 15 when the tracheal tree formed at 3 hours intervals.

Cigarette smoke and hypoxic exposure

All cigarette smoke exposure experiments were carried out in a smoking chamber, attached to a diaphragm pump. Common research 3R4F cigarettes (CTRP, Kentucky University, Lexington, USA) were used for all experiments. The vials containing animals were capped with a monitoring grid to allow the cigarette smoke to diffuse into the vial. For long-time smoke experiments, L2 larvae were exposed to smoke three times a day for 30 min each, on two consecutive days. For heavy smoke experiments, L3 larvae were exposed to 2 cigarettes smoke one time for 45 min, which led to about 35-50% mortality. To study the effects of hypoxia on the activity of JAK/STAT signalling pathway, larvae were exposed to long-term hypoxia and short-term hypoxia separately. For long-term hypoxia experiments, L2 larvae were exposed to 5% oxygen three times a day for 30 min each, on two consecutive days. For short-term hypoxia experiments, L3 larvae were exposed to 1% oxygen once for 5 hours.

Antibody and tracheal stains

Larvae were dissected by ventral filleting and fixed in 4% paraformaldehyde for 30 min. Embryos were staged according to Campos-Ortega and Hartenstein [69] and fixed in 4% formaldehyde for 30 min. Immunostaining followed standard protocols as described earlier [70, 71]. GFP signals were amplified by immunostaining with polyclonal rabbit anti-GFP (used at 1:500, Sigma-Aldrich, Merck KGaA, Darmstadt, Germany, SAB4301138). 40-1a (used at 1:50, DSHB, Iowa City, USA) was used to detect Beta-galactosidase. Coracle protein was detected with a monoclonal mouse anti-coracle antibody (used at 1:200,

DSHB, Iowa City, USA, C566.9). Armadillo protein was detected with a monoclonal mouse anti-armadillo antibody (DSHB, US, N2 7A1, used at 1:500). A monoclonal rabbit Cleaved Drosophila Dcp1 (used at 1:200, Cell Signaling, Frankfurt/M, Germany, #9578) was used to detect apoptotic cells. Secondary antibodies used were: Cy3-conjugated goat-anti-mouse, Cy3-conjugated goat-anti-rabbit, Alexa488-conjugated goat-anti-mouse (Jackson Immunoresearch, Dianova, Hamburg, Germany), Alexa488-conjugated goat-anti-rabbit (used at 1:500, Cell signaling, Frankfurt/M, Germany, #9578). Tracheal chitin was stained with 505 star conjugated chitin-binding probe (NEB, Germany, used at 1:300). Nuclei were stained with 4',6-Diamidino-2-Phenylindole, Dihydrochloride (DAPI) (Roth, Karlsruhe, Germany, 6843). Specimens were analyzed and digital images captured either with a confocal (CLSM Leica TCS SP1, Leica, Wetzlar, Germany) or a conventional fluorescence microscope (ZEISS Axio Imager Z1, Zeiss, Oberkochen, Germany), respectively.

RNA isolation and RNA sequencing

For the gene expression analysis of 3rd instar larvae trachea, animals were dissected in cold PBS and isolated trachea transferred to RNA Magic (BioBudget, Krefeld, Germany) and processed essentially as described earlier [60] with slight modifications. The tissue was homogenized in a Bead Ruptor 24 (BioLab products, Bebensee, Germany) and the RNA was extracted by using the PureLink RNA Mini Kit (Thermo Fisher, Waltham, MA, USA) for phase separation with the RNA Magic reagent. An additional DNase treatment was

464 performed following the on-column PureLink DNase treatment protocol (Thermo Fisher,
465 Waltham, MA, USA).
466 Sequencing libraries were constructed using the TruSeq stranded mRNA kit (Illumina, San
467 Diego, USA) and 50 bp single-read sequencing was performed on an Illumina HiSeq 4000
468 with 16 samples per lane. Resulting sequencing reads were trimmed for low-quality bases
469 and adapters using the fastq Illumina filter
470 (http://cancan.cshl.edu/labmembers/gordon/fastq_illumina_filter/) and cutadapt
471 (version 1.8.1) [72]. Transcriptomics analysis including gene expression values and
472 differential expression analysis was done using CLC Genomics Workbench. The detailed
473 protocols can be obtained from the CLC Web site (http://www. clcbio.com/products/clc-
474 genomics-workbench). *Drosophila melanogaster* reference genome (Release 6) [73] was
475 used for mapping in this research.
476 The transcription factor binding site enrichment and the Gene Ontology enrichment
477 analyses of the differentially expressed genes were carried out using Pscan and Panther,
478 respectively. Date was visualized through the circos software.
479

480 ## References

481
482 1. Rawlings JS, Rosler KM, Harrison DA: **The JAK/STAT signaling pathway**. *J Cell Sci* 2004, **117**(Pt
483 8):1281-1283.
484 2. Zeidler MP, Bausek N: **The Drosophila JAK-STAT pathway**. *JAKSTAT* 2013, **2**(3):e25353.
485 3. Yan R, Small S, Desplan C, Dearolf CR, Darnell JE, Jr.: **Identification of a Stat gene that functions in**
486 **Drosophila development**. *Cell* 1996, **84**(3):421-430.

4. Shuai K, Liu B: **Regulation of JAK-STAT signalling in the immune system**. *Nat Rev Immunol* 2003, **3**(11):900-911.
5. Villarino AV, Kanno Y, Ferdinand JR, O'Shea JJ: **Mechanisms of Jak/STAT signaling in immunity and disease**. *J Immunol* 2015, **194**(1):21-27.
6. Villarino AV, Kanno Y, O'Shea JJ: **Mechanisms and consequences of Jak-STAT signaling in the immune system**. *Nat Immunol* 2017, **18**(4):374-384.
7. Agaisse H, Perrimon N: **The roles of JAK/STAT signaling in Drosophila immune responses**. *Immunol Rev* 2004, **198**:72-82.
8. O'Shea JJ, Schwartz DM, Villarino AV, Gadina M, McInnes IB, Laurence A: **The JAK-STAT pathway: impact on human disease and therapeutic intervention**. *Annu Rev Med* 2015, **66**:311-328.
9. Constantinescu SN, Girardot M, Pecquet C: **Mining for JAK-STAT mutations in cancer**. *Trends Biochem Sci* 2008, **33**(3):122-131.
10. Pernis AB, Rothman PB: **JAK-STAT signaling in asthma**. *J Clin Invest* 2002, **109**(10):1279-1283.
11. Tadokoro T, Wang Y, Barak LS, Bai Y, Randell SH, Hogan BL: **IL-6/STAT3 promotes regeneration of airway ciliated cells from basal stem cells**. *Proc Natl Acad Sci U S A* 2014, **111**(35):E3641-3649.
12. Kida H, Mucenski ML, Thitoff AR, Le Cras TD, Park KS, Ikegami M, Muller W, Whitsett JA: **GP130-STAT3 regulates epithelial cell migration and is required for repair of the bronchiolar epithelium**. *Am J Pathol* 2008, **172**(6):1542-1554.
13. Dutta P, Sabri N, Li J, Li WX: **Role of STAT3 in lung cancer**. *JAKSTAT* 2014, **3**(4):e999503.
14. Arbouzova NI, Zeidler MP: **JAK/STAT signalling in Drosophila: insights into conserved regulatory and cellular functions**. *Development* 2006, **133**(14):2605-2616.
15. Brown S, Hu N, Hombria JC: **Identification of the first invertebrate interleukin JAK/STAT receptor, the Drosophila gene domeless**. *Curr Biol* 2001, **11**(21):1700-1705.
16. Perrimon N, Mahowald AP: **l(1)hopscotch, A larval-pupal zygotic lethal with a specific maternal effect on segmentation in Drosophila**. *Dev Biol* 1986, **118**(1):28-41.
17. Harrison DA, McCoon PE, Binari R, Gilman M, Perrimon N: **Drosophila unpaired encodes a secreted protein that activates the JAK signaling pathway**. *Genes Dev* 1998, **12**(20):3252-3263.
18. Isaac DD, Andrew DJ: **Tubulogenesis in Drosophila: a requirement for the trachealess gene product**. *Genes Dev* 1996, **10**(1):103-117.
19. Nogueira-Silva C, Santos M, Baptista MJ, Moura RS, Correia-Pinto J: **IL-6 is constitutively expressed during lung morphogenesis and enhances fetal lung explant branching**. *Pediatr Res* 2006, **60**(5):530-536.
20. Piairo P, Moura RS, Baptista MJ, Correia-Pinto J, Nogueira-Silva C: **STATs in Lung Development: Distinct Early and Late Expression, Growth Modulation and Signaling Dysregulation in Congenital Diaphragmatic Hernia**. *Cell Physiol Biochem* 2018, **45**(1):1-14.
21. Bach EA, Ekas LA, Ayala-Camargo A, Flaherty MS, Lee H, Perrimon N, Baeg GH: **GFP reporters detect the activation of the Drosophila JAK/STAT pathway in vivo**. *Gene Expr Patterns* 2007, **7**(3):323-331.
22. Shiga Y, M. TM, Hayashi S: **A nuclear GFP/ β - galactosidase fusion protein as a marker for morphogenesis in living Drosophila**. *Development, Growth & Differentiation* 1996, **38**:99-106.

23. Roskoski R, Jr.: **Janus kinase (JAK) inhibitors in the treatment of inflammatory and neoplastic diseases**. *Pharmacol Res* 2016, **111**:784-803.
24. Lindsay SA, Lin SJH, Wasserman SA: **Short-Form Bomanins Mediate Humoral Immunity in Drosophila**. *J Innate Immun* 2018, **10**(4):306-314.
25. Lock JG, Stow JL: **Rab11 in recycling endosomes regulates the sorting and basolateral transport of E-cadherin**. *Mol Biol Cell* 2005, **16**(4):1744-1755.
26. Oshima K, Fehon RG: **Analysis of protein dynamics within the septate junction reveals a highly stable core protein complex that does not include the basolateral polarity protein Discs large**. *J Cell Sci* 2011, **124**(Pt 16):2861-2871.
27. Jayaram SA, Senti KA, Tiklova K, Tsarouhas V, Hemphala J, Samakovlis C: **COPI vesicle transport is a common requirement for tube expansion in Drosophila**. *PLoS One* 2008, **3**(4):e1964.
28. Tsarouhas V, Senti KA, Jayaram SA, Tiklova K, Hemphala J, Adler J, Samakovlis C: **Sequential pulses of apical epithelial secretion and endocytosis drive airway maturation in Drosophila**. *Dev Cell* 2007, **13**(2):214-225.
29. Glasheen BM, Robbins RM, Piette C, Beitel GJ, Page-McCaw A: **A matrix metalloproteinase mediates airway remodeling in Drosophila**. *Dev Biol* 2010, **344**(2):772-783.
30. Liu L, Johnson WA, Welsh MJ: **Drosophila DEG/ENaC pickpocket genes are expressed in the tracheal system, where they may be involved in liquid clearance**. *Proc Natl Acad Sci U S A* 2003, **100**(4):2128-2133.
31. Wagner C, Isermann K, Roeder T: **Infection induces a survival program and local remodeling in the airway epithelium of the fly**. *Faseb J* 2009, **23**(7):2045-2054.
32. Kode A, Yang SR, Rahman I: **Differential effects of cigarette smoke on oxidative stress and proinflammatory cytokine release in primary human airway epithelial cells and in a variety of transformed alveolar epithelial cells**. *Respir Res* 2006, **7**:132.
33. Hombria JC, Sotillos S: **JAK-STAT pathway in Drosophila morphogenesis: From organ selector to cell behavior regulator**. *JAKSTAT* 2013, **2**(3):e26089.
34. Powers N, Srivastava A: **JAK/STAT signaling is involved in air sac primordium development of Drosophila melanogaster**. *FEBS Lett* 2019, **593**(7):658-669.
35. Zheng XJ, Yang ZX, Dong YJ, Zhang GY, Sun MF, An XK, Pan LH, Zhang SL: **Downregulation of leptin inhibits growth and induces apoptosis of lung cancer cells via the Notch and JAK/STAT3 signaling pathways**. *Biol Open* 2016, **5**(6):794-800.
36. Quinton LJ, Mizgerd JP: **NF-kappaB and STAT3 signaling hubs for lung innate immunity**. *Cell Tissue Res* 2011, **343**(1):153-165.
37. Matsuzaki Y, Xu Y, Ikegami M, Besnard V, Park KS, Hull WM, Wert SE, Whitsett JA: **Stat3 is required for cytoprotection of the respiratory epithelium during adenoviral infection**. *J Immunol* 2006, **177**(1):527-537.
38. Hokuto I, Ikegami M, Yoshida M, Takeda K, Akira S, Perl AK, Hull WM, Wert SE, Whitsett JA: **Stat-3 is required for pulmonary homeostasis during hyperoxia**. *J Clin Invest* 2004, **113**(1):28-37.
39. Jiang H, Patel PH, Kohlmaier A, Grenley MO, McEwen DG, Edgar BA: **Cytokine/Jak/Stat signaling mediates regeneration and homeostasis in the Drosophila midgut**. *Cell* 2009, **137**(7):1343-1355.

40. Miguel-Aliaga I, Jasper H, Lemaitre B: **Anatomy and Physiology of the Digestive Tract of Drosophila melanogaster**. *Genetics* 2018, **210**(2):357-396.
41. Simeone-Penney MC, Severgnini M, Tu P, Homer RJ, Mariani TJ, Cohn L, Simon AR: **Airway epithelial STAT3 is required for allergic inflammation in a murine model of asthma**. *J Immunol* 2007, **178**(10):6191-6199.
42. Zhang X, Yue P, Page BD, Li T, Zhao W, Namanja AT, Paladino D, Zhao J, Chen Y, Gunning PT *et al*: **Orally bioavailable small-molecule inhibitor of transcription factor Stat3 regresses human breast and lung cancer xenografts**. *Proc Natl Acad Sci U S A* 2012, **109**(24):9623-9628.
43. Yew-Booth L, Birrell MA, Lau MS, Baker K, Jones V, Kilty I, Belvisi MG: **JAK-STAT pathway activation in COPD**. *Eur Respir J* 2015, **46**(3):843-845.
44. Prele CM, Yao E, O'Donoghue RJ, Mutsaers SE, Knight DA: **STAT3: a central mediator of pulmonary fibrosis?** *Proc Am Thorac Soc* 2012, **9**(3):177-182.
45. Gao H, Guo RF, Speyer CL, Reuben J, Neff TA, Hoesel LM, Riedemann NC, McClintock SD, Sarma JV, Van Rooijen N *et al*: **Stat3 activation in acute lung injury**. *J Immunol* 2004, **172**(12):7703-7712.
46. Liu RY, Zeng Y, Lei Z, Wang L, Yang H, Liu Z, Zhao J, Zhang HT: **JAK/STAT3 signaling is required for TGF-beta-induced epithelial-mesenchymal transition in lung cancer cells**. *Int J Oncol* 2014, **44**(5):1643-1651.
47. Fahy JV, Dickey BF: **Airway mucus function and dysfunction**. *N Engl J Med* 2010, **363**(23):2233-2247.
48. Georas SN, Rezaee F: **Epithelial barrier function: at the front line of asthma immunology and allergic airway inflammation**. *J Allergy Clin Immunol* 2014, **134**(3):509-520.
49. Gon Y, Hashimoto S: **Role of airway epithelial barrier dysfunction in pathogenesis of asthma**. *Allergol Int* 2018, **67**(1):12-17.
50. Heijink IH, Brandenburg SM, Postma DS, van Oosterhout AJ: **Cigarette smoke impairs airway epithelial barrier function and cell-cell contact recovery**. *Eur Respir J* 2012, **39**(2):419-428.
51. Milara J, Ballester B, Morell A, Ortiz JL, Escriva J, Fernandez E, Perez-Vizcaino F, Cogolludo A, Pastor E, Artigues E *et al*: **JAK2 mediates lung fibrosis, pulmonary vascular remodelling and hypertension in idiopathic pulmonary fibrosis: an experimental study**. *Thorax* 2018, **73**(6):519-529.
52. Athari SS: **Targeting cell signaling in allergic asthma**. *Signal Transduct Target Ther* 2019, **4**:45.
53. Loh CY, Arya A, Naema AF, Wong WF, Sethi G, Looi CY: **Signal Transducer and Activator of Transcription (STATs) Proteins in Cancer and Inflammation: Functions and Therapeutic Implication**. *Front Oncol* 2019, **9**:48.
54. Severgnini M, Takahashi S, Rozo LM, Homer RJ, Kuhn C, Jhung JW, Perides G, Steer M, Hassoun PM, Fanburg BL *et al*: **Activation of the STAT pathway in acute lung injury**. *Am J Physiol Lung Cell Mol Physiol* 2004, **286**(6):L1282-1292.
55. Song L, Rawal B, Nemeth JA, Haura EB: **JAK1 activates STAT3 activity in non-small-cell lung cancer cells and IL-6 neutralizing antibodies can suppress JAK1-STAT3 signaling**. *Mol Cancer Ther* 2011, **10**(3):481-494.
56. Andrew DJ, Ewald AJ: **Morphogenesis of epithelial tubes: Insights into tube formation, elongation, and elaboration**. *Dev Biol* 2010, **341**(1):34-55.

57. Bergman P, Seyedoleslami Esfahani S, Engstrom Y: **Drosophila as a Model for Human Diseases-Focus on Innate Immunity in Barrier Epithelia**. *Curr Top Dev Biol* 2017, **121**:29-81.
58. Bossen J, Uliczka K, Steen L, Pfefferkorn R, Mai MM, Burkhardt L, Spohn M, Bruchhaus I, Fink C, Heine H *et al*: **An EGFR-Induced Drosophila Lung Tumor Model Identifies Alternative Combination Treatments**. *Mol Cancer Ther* 2019, **18**(9):1659-1668.
59. Levine BD, Cagan RL: **Drosophila Lung Cancer Models Identify Trametinib plus Statin as Candidate Therapeutic**. *Cell Rep* 2016, **14**(6):1477-1487.
60. Prange R, Thiedmann M, Bhandari A, Mishra N, Sinha A, Hasler R, Rosenstiel P, Uliczka K, Wagner C, Yildirim AO *et al*: **A Drosophila model of cigarette smoke induced COPD identifies Nrf2 signaling as an expedient target for intervention**. *Aging (Albany NY)* 2018, **10**(8):2122-2135.
61. Kallsen K, Zehethofer N, Abdelsadik A, Lindner B, Kabesch M, Heine H, Roeder T: **ORMDL deregulation increases stress responses and modulates repair pathways in Drosophila airways**. *J Allergy Clin Immunol* 2015, **136**(4):1105-1108.
62. Roeder T, Isermann K, Kabesch M: **Drosophila in asthma research**. *Am J Respir Crit Care Med* 2009, **179**(11):979-983.
63. Roeder T, Isermann K, Kallsen K, Uliczka K, Wagner C: **A Drosophila asthma model - what the fly tells us about inflammatory diseases of the lung**. *Adv Exp Med Biol* 2012, **710**:37-47.
64. Brand AH, Perrimon N: **Targeted gene expression as a means of altering cell fates and generating dominant phenotypes**. *Development* 1993, **118**(2):401-415.
65. Harrison DA, Binari R, Nahreini TS, Gilman M, Perrimon N: **Activation of a Drosophila Janus kinase (JAK) causes hematopoietic neoplasia and developmental defects**. *EMBO J* 1995, **14**(12):2857-2865.
66. Fink C, Hoffmann J, Knop M, Li Y, Isermann K, Roeder T: **Intestinal FoxO signaling is required to survive oral infection in Drosophila**. *Mucosal Immunol* 2016, **9**(4):927-936.
67. Bosch JA, Tran NH, Hariharan IK: **CoinFLP: a system for efficient mosaic screening and for visualizing clonal boundaries in Drosophila**. *Development* 2015, **142**(3):597-606.
68. Chen F, Krasnow MA: **Progenitor outgrowth from the niche in Drosophila trachea is guided by FGF from decaying branches**. *Science* 2014, **343**(6167):186-189.
69. Campos-Ortega JA, Hartenstein V: **The Embryonic Development of Drosophila melanogaster**: Springer-Verlag Berlin Heidelberg; 1997.
70. Jeon M, Nguyen H, Bahri S, Zinn K: **Redundancy and compensation in axon guidance: genetic analysis of the Drosophila Ptp10D/Ptp4E receptor tyrosine phosphatase subfamily**. *Neural Dev* 2008, **3**:3.
71. Levi BP, Ghabrial AS, Krasnow MA: **Drosophila talin and integrin genes are required for maintenance of tracheal terminal branches and luminal organization**. *Development* 2006, **133**(12):2383-2393.
72. Martin M: **Cutadapt Removes Adapter Sequences From High-Throughput Sequencing Reads**. *EMBnetjournal* 2011, **17**:10-12.
73. Hoskins RA, Carlson JW, Wan KH, Park S, Mendez I, Galle SE, Booth BW, Pfeiffer BD, George RA, Svirskas R *et al*: **The Release 6 reference sequence of the Drosophila melanogaster genome**. *Genome Res* 2015, **25**(3):445-458.

649

650 Table 1 Genes that were most strongly upregulated in response to Hop.CA
651 overexpression.

Name	Maximum group mean	Fold change	FDR p-value
CG16772	11.85472435	135.4356918	0
hop	286.0640796	35.42957686	0
CG14570	42.20996514	35.3698493	0
CG14147	55.30940549	32.87679686	0
Hsp70Bb	161.511126	29.98530152	0
Ubx	200.4588187	23.51089416	0
pre-mod(mdg4)-I	1.124681971	18.66759173	2.22648E-06
IM14	11.45782606	15.13546529	3.80132E-07
IM4	26.42664387	14.97315552	1.74645E-12
CG14569	1576.880077	14.72575164	0
IM2	7.261319979	14.4714161	2.01792E-06
CG5791	1.786460103	13.80267454	2.90502E-05
CG9121	3.412245019	11.53962271	0
IM1	7.159415315	10.97306621	7.52122E-05
CG11413	35.69960698	10.63636792	3.44242E-07
CG16710	2.132413445	10.32026533	1.72352E-07
CG31960	267.2645814	10.04792875	0
CG16789	1.452007625	9.460811492	5.58576E-09
CG6034	6.915088882	8.468387575	4.7943E-11
Ace	2.056513226	8.187696842	0
CG13059	9.898481009	7.578675956	1.33893E-06
CG31809	8.642528741	7.388263435	0
CG7203	9.406607055	7.213889526	8.66989E-09
Vha14-2	2.510881225	7.050881817	2.31024E-07
wb	7.35456153	6.689915209	0
Drs	8166.473129	6.635790672	0
CG5778	3.202417196	6.607038471	0.000294835
CG3457	2.693960701	6.337465056	2.38755E-06
Lcp65Ad	9.932204556	5.792567795	2.58249E-08
lectin-22C	29.06148461	5.674130819	6.88538E-06
fuss	3.973734058	5.673577323	0

CG43333	2.390923691	5.632143859	1.48392E-09
CG18336	2.963052606	5.485479621	5.52167E-05
CG32563	3.062298877	5.352654098	0.000696584
FASN2	1.651227873	5.340581227	2.95545E-10
Cyp4d21	45.69613978	5.308508635	0
Obp57d	1.797549513	5.276761495	0.000102926
CG17560	2.313559171	5.218521032	0.000766701
CG5888	68.16302548	5.201444372	0

652 $p < 1\times10^{-4}$, fold change > 5, maximum group mean > 1. The list is restricted to 39 genes.

653

654 Table 2 Transcription factor-binding site motifs enriched in 41 highly upregulated genes.

Matrix ID	Matrix name	P-value
MA0023.1	dl (var.2)	0.000443261
MA0022.1	dl	0.00407113
MA0532.1	Stat92E	0.00794732
MA0450.1	hkb	0.00811969
MA0197.2	nub	0.0154201
MA0242.1	Bgb::run	0.0371696
MA0204.1	Six4	0.0443521
MA0444.1	CG34031	0.0488169

655 A total of 133 transcription factor profiles were used.

656

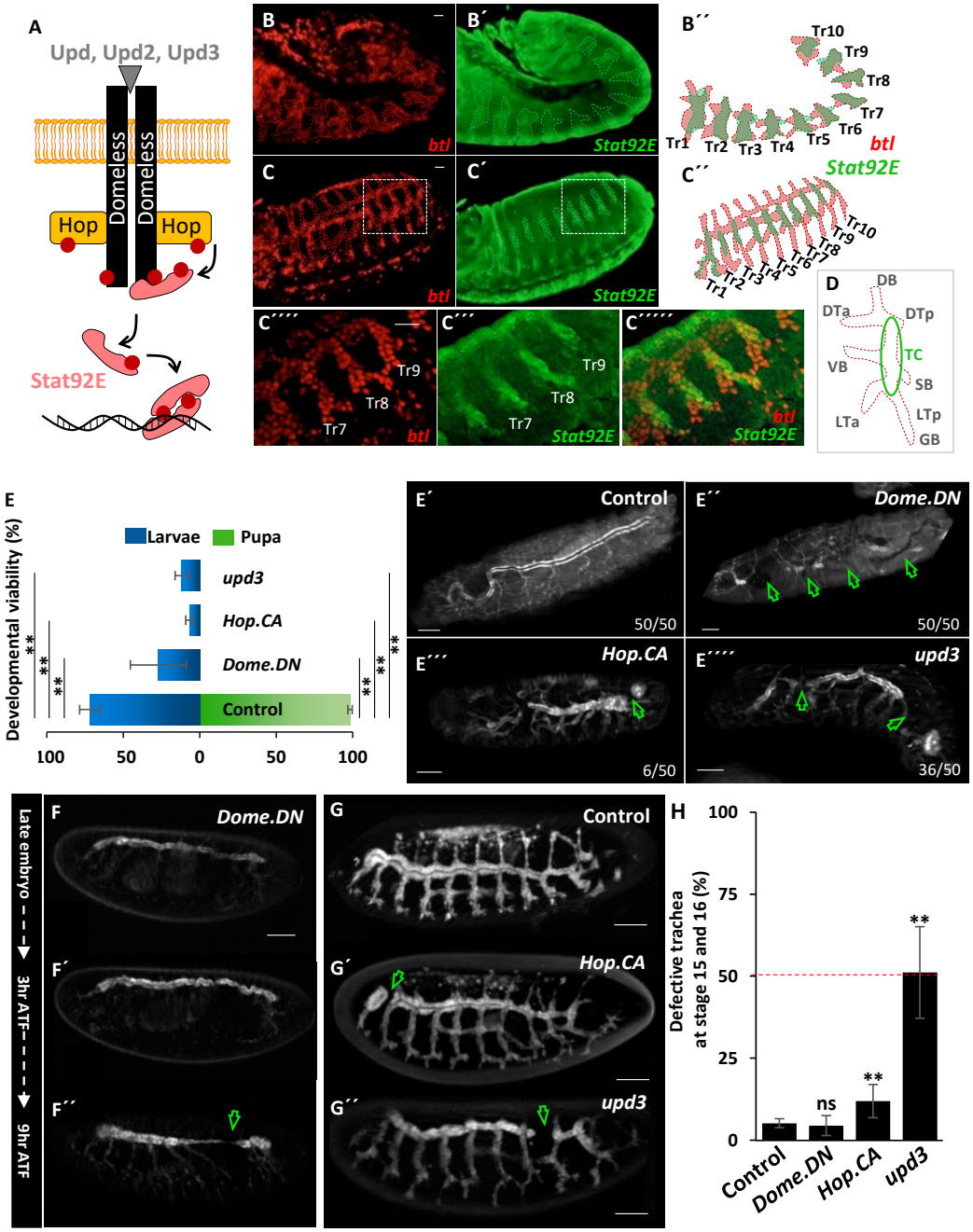

657

658 Figure 1: Effects of JAK/STAT signaling in the airway development in *Drosophila* embryos. (A) shows a
659 model of JAK/STAT signaling pathway in *Drosophila* comprising all major components. Three ligands
660 (Upd, Upd2 and Upd3) bind to a single receptor, Domeless (Dome), which transmits this information
661 via a single JAK (Hopscotch (Hop)) to a single STAT transcription factor (Stat92E). (B-D) Fluorescence
662 micrographs of *btl-Gal4*; *Stat92E-GFP*; *UAS-LacZ.nls* embryos stained for GFP (green, JAK/STAT pathway
663 activated zones), Beta-galactosidase (red, tracheal metamere), respectively. The JAK/STAT signaling
664 pathway is activated in the whole trachea metamere (Tr). The activation of JAK/STAT pathway in the

terminal regions is weaker than that in the central regions before (B) and after the fuse of tracheal invaginations of all segments (C). (D) shows the pattern of activation of JAK/STAT signaling in the trachea metamere of embryos. DB, dorsal branch; DTa, dorsal trunk anterior; DTp, dorsal trunk posterior; VB, visceral branch; LTa, lateral trunk anterior; LTp, lateral trunk posterior; and GB, ganglionic branch; SB, spiracular branch; transverse connective, TC. The stronger signal in the central regions mainly belongs to TC. Scale bar: 20 μm. (E) Ectopic blocking or activation of JAK/STAT signaling in the trachea was done by expressing of *Dome.DN* or *Hop.CA* (or *upd3*), respectively under the control of *btl-Gal4*. The percentage of embryos that hatched and the percentage of larva that developed into pupa is shown at the left side. Right (E'-E''''): Micrographs surviving larvae. *Btl* driving the expression of *upd3* and *Dome.DN* inhibited the formation of an intact tracheal tree. *Btl* driving the expression of *Hop.CA* in the trachea showed more intact trachea trees compared to expressing *upd3* and *Dome.DN* in the trachea. X/XX: broken trachea/intact trachea; 50 animals were observed in each group. (F) Time-lapse imaging the trachea of *btl>Dome.DN* embryo continuously for 9 hours after the trachea formed (9hr ATF). 40 specimens were investigated. (G-H) Activation of the JAK/STAT pathway in the trachea led to incompleted tracheal development during tracheal morphogenesis. Fluorescence micrographs of *btl>Hop.CA* (or >*upd3*) embryos (G), and numbers of the trachea which had no fused Tr. (H) Quantification of the numbers of defect tracheal branches in response to the different treatments. Each group contains 3 replicates and each replicate contains 30 embryos in G and H. Arrows mark the broken sites in the trachea. ns means not significant, * $p < 0.05$, ** $p < 0.01$ by Student's t-test. Scale bar: 20 μm in B-D; 50 μm in E-G.

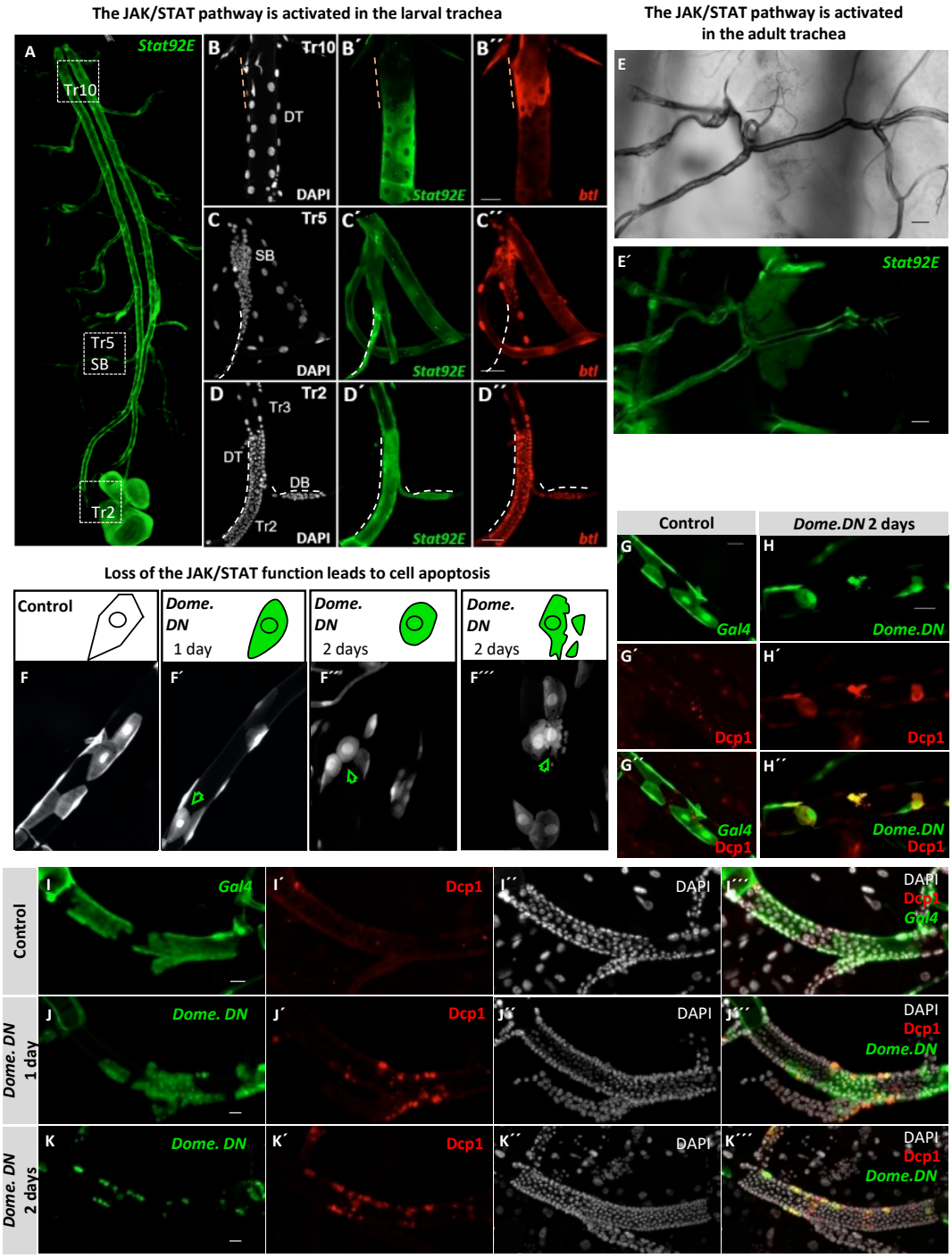

Figure 2: Inhibition of JAK/STAT signaling pathway induced cell apoptosis. (A-D) Fluorescence micrographs of *btl-Gal4; Stat92E-GFP*; *UAS-LacZ.nls* larvae. The activation of JAK/STAT signaling was detected by using the *Stat92E-GFP* reporter. In general, JAK/STAT signaling was induced in the whole trachea of the larvae. The region in the posterior region of the trachea (orange dash line in B) that is going to degenerate will lose JAK/STAT signaling. Conversely, some regions like Tr2, DB (C), and SB (D)

where the cell re-enter into cell cycle (white dash line) exhibited stronger JAK/STAT signaling compared to the cell quiescent areas close to them. (E) Fluorescence micrographs of *btl-Gal4; Stat92E-GFP*; *UAS-LacZ.nls* adult. JAK/STAT signaling was induced in the trachea of the adult. (F) Fluorescence micrographs of the mutant clones in the trachea of *vvl-FLP*, *CoinFLP-Gal4, UAS-EGFP; tub-Gal80[ts]* (*vvl-coin.ts*)*>UAS-Dome.DN* larvae. Negative regulation of JAK/STAT pathway by expressing *Dome.DN* in the trachea led to the loss of cell shape and disintegration afterward (green arrows). (G-K) Fluorescence micrographs of the trachea of *vvl-coin.ts* larvae (G), and the trachea of *vvl-coin.ts>UAS-Dome.DN* larvae (H) stained for cleaved Dcp1 (red). Modified stem cells (J and K) could be stained by cleaved Dcp1 earlier than the mutant somatic cells. Inhibition of JAK/STAT signaling induced blockade of cell division (I and K). 50 specimens were used in each assay.

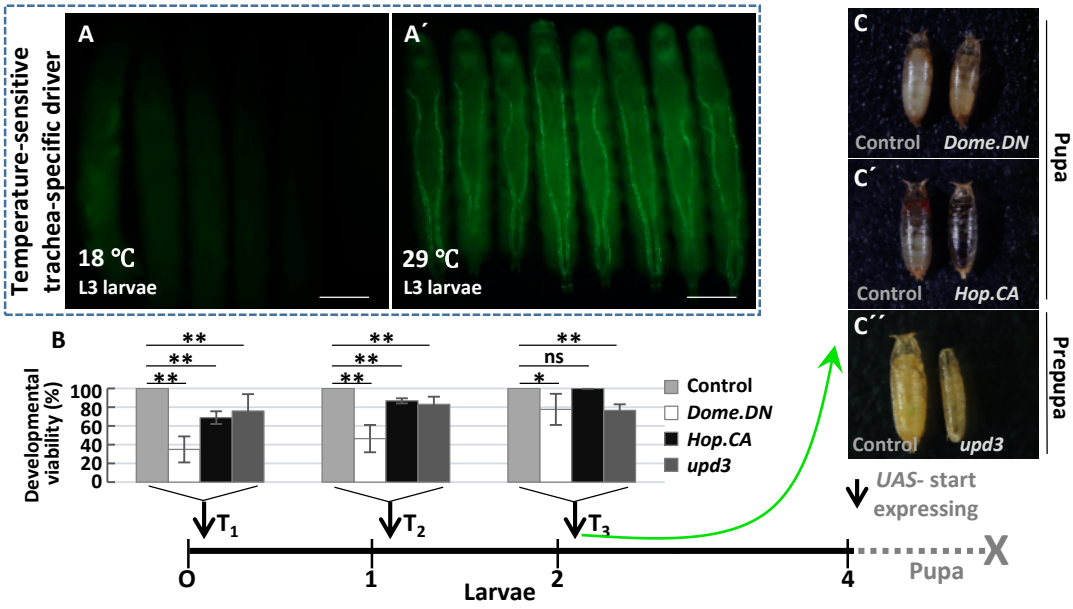

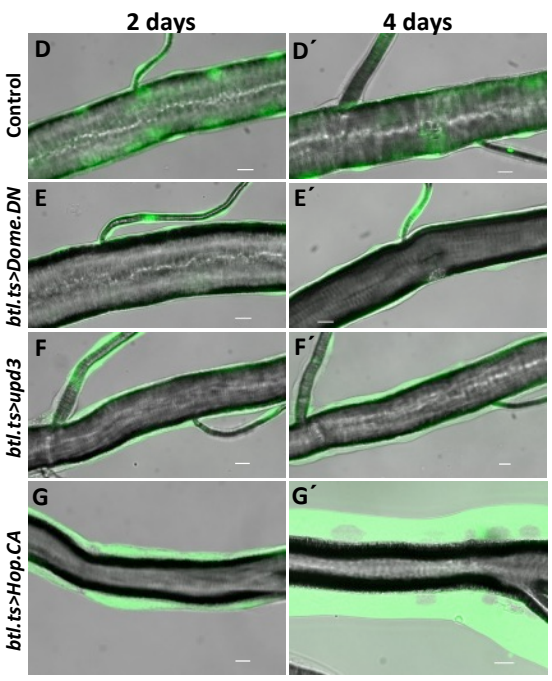

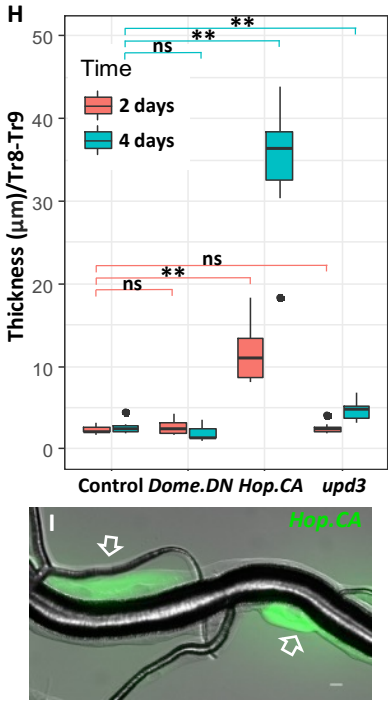

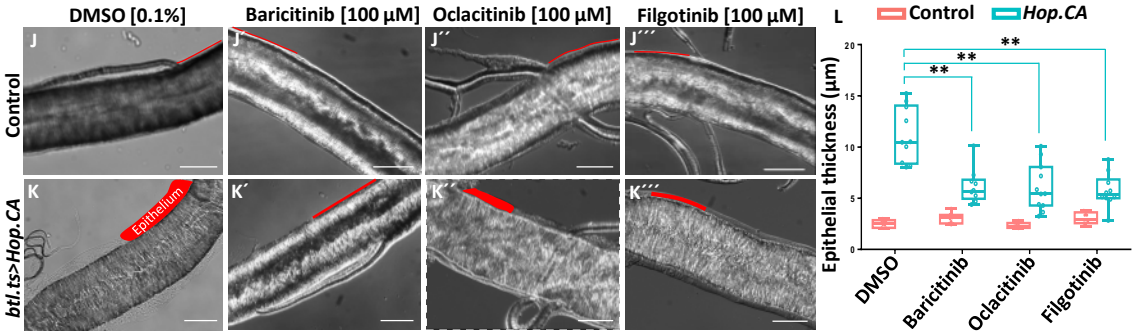

703

Figure 3: Ectopic activation of epithelial JAK/STAT signaling induces cell thickening. (A) *btl-Gal4, UAS-GFP; tub-Gal80[ts]* (*btl.ts*) larvae were reared at 18 ℃ (nonpermissive, A) and 29 ℃ (permissive, A´), respectively. Using the Gal4/UAS system, comprising the temperature-sensitive repressor Gal80[ts], were used to time ectopic gene expression. (B) Developmental viability of larvae with different genotypes (including *Dome.DN*, *Hop.CA*, and *upd3* expression in the trachea driven by *btl.ts*) and different start points of expression (indicated by black arrows). Statistical analysis of survival times is included. In this experiment, 4 replicates were performed with 30 larvae in B. (C) In general, none of these manipulations allowed survival up to adults. (D-G) Micrographs of Tr8-Tr9 of *btl.ts* L3 larvae (D, Control); *btl.ts>Dome.DN* L3 larvae (E); *btl.ts>Hop.CA* L3 larvae (F) and *btl.ts>upd3* L3 larvae (G) that were raised at 29 ℃ for 2 and 4 days, respectively. (H) Statistical analysis of the epithelial thicknesses in Tr8-Tr9 of the corresponding larvae. The thickness of 30 trachea per group were measured in H. (I) Micrographs of Tr8 of *vvl-FLP*, *CoinFLP-Gal4, UAS-EGFP* (*vvl-coin*)*>UAS-Hop.CA* larvae. The thickening of the tracheal epithelium is observed in those cells that express *Hop.CA*. Changes in epithelial thickness could be rescued by application of specific JAK inhibitors (J-L). (J-K) Microscopy of the tracheal epithelium (L3 larvae). Control crossings *btl.ts>w*^{1118} (J) compared to JAK/STAT activated crossings *btl.ts>UAS-Hop.CA* (K). (L) Illustration and quantification of epithelial thickness (highlighted in red) of the JAK inhibitors (Baricitinib, Oclacitinib, Filgotinib) compared to DMSO control. The thickness of 10 trachea per group were measured in J,K. ns means no significant, * $p < 0.05$, ** $p < 0.01$ by Student's t-test. Scale bar: 500 µm in A; 20 µm in D-G; 50 µm J-K.

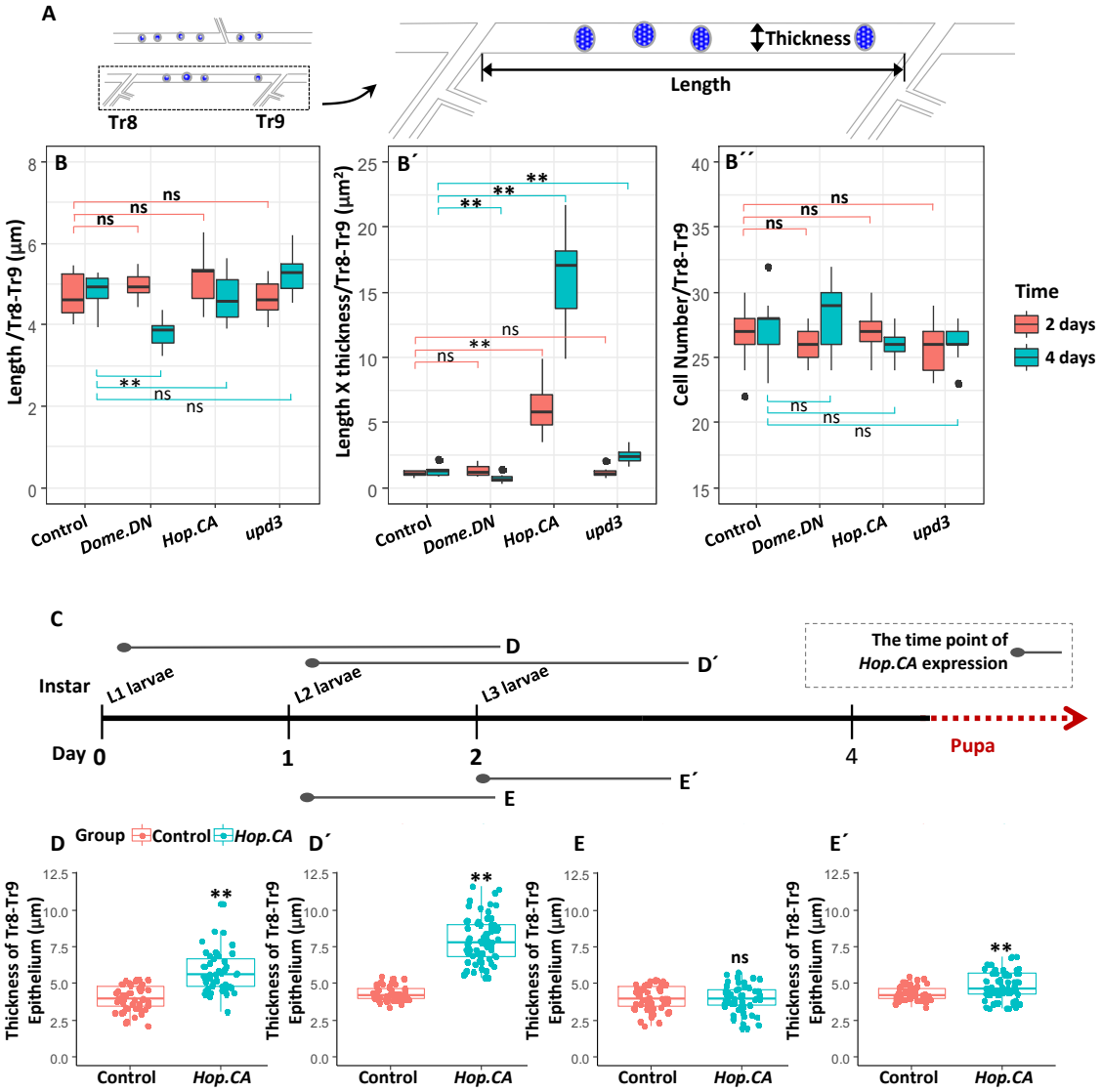

Figure 4: Changes in epithelial thickness could be attributed to the increase in cell volume and is time-dependent. (A-B) Illustration and quantification of the length, length X thickness, and the cell number of the Tr8-Tr9 region of larvae with different types of ectopic manipulation (including *Dome.DN*, *Hop.CA* and *upd3* expression in the trachea driven by *btl.ts*) for 2 or 4 days, respectively. 30 trachea were analysed in each group. (C-E) Illustration of the time point and period of activation of *Hop.CA* expression by using the *btl.ts* (C) and quantification of the thickness of the Tr8-Tr9 region of control larvae (*btl.ts* line) and those experiencing ectopic manipulation (*btl.ts>Hop.CA* line). Quantitative analyses of the thicknesses (D). 1-day expression of *Hop.CA* starting at L2 larvae (E), but that started at the early L3 stage promotes epithelial thickening (E´). Each group contains 50 replicates in D-E. ns means not significant, * $p < 0.05$, ** $p < 0.01$ by Student's t-test.

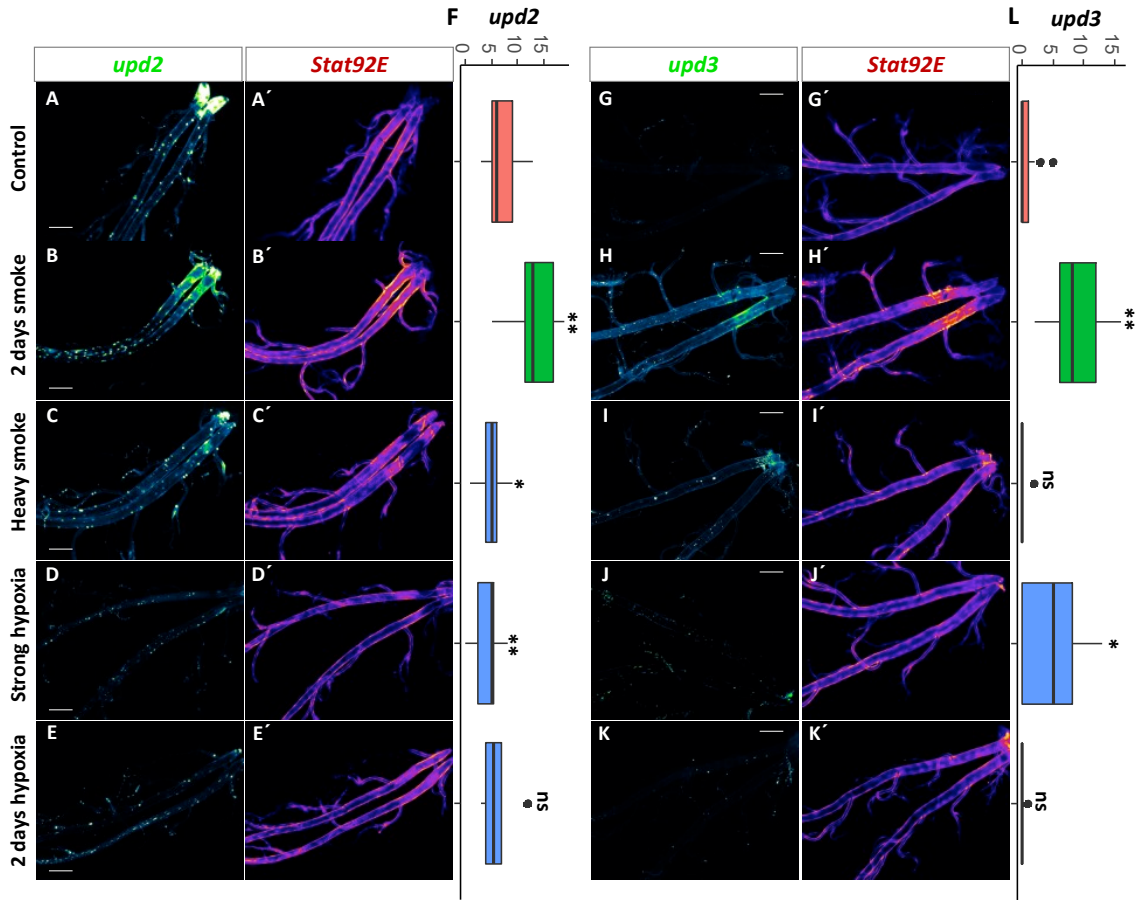

Figure 5: JAK/STAT signaling in airway epithelial cells is activated by long term cigarette smoke exposure. Fluorescence micrographs of the trachea of *upd2* (A-E) or *upd3* (G-K)-*Gal4*; *Stat92E-GFP*; *UAS-LacZ.nls* larvae that were exposed for 2 days smoke (B and H), heavy smoke (C and I), strong hypoxia (D and J), and 2 days of hypoxia (E and K). Trachea were stained for GFP (red, JAK/STAT pathway activated zones), Beta-galactosidase (green, cells that expressed upd2 and upd3), respectively. (F and L) The numbers of cells that expressed *upd2* and *upd3* were counted under these different conditions. 40 trachea in each group were assayed. ns means not significant, * $p < 0.05$, ** $p < 0.01$ by Student's t-test. Scale bar: 200 µm.

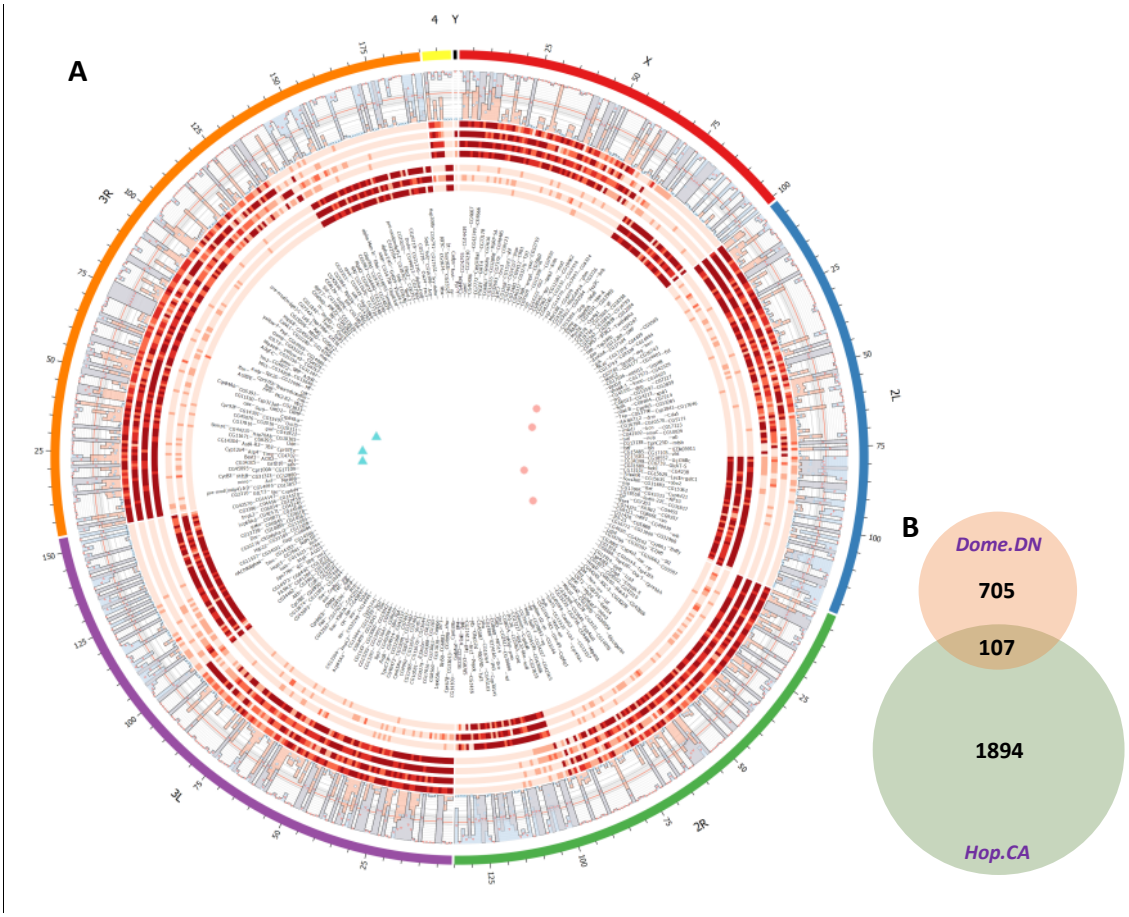

Figure 6: Changes at the transcript level in the airway epithelium of JAK/STAT mutants. Altered gene expression levels in the trachea caused by 16 hours persistent expression of *Hop.CA* driven by *btl.ts*. In total, 2004 genes were regulated significantly ($p < 0.05$), in which 707 genes of (fold change > 2, $p < 0.01$) showing even higher levels of significance. (A) These 707 genes were used to visualize the differences of the transcript levels between *Hop.CA* expressed trachea and control trachea. From the outside to the inside, a histogram for expression mean values (red, control; blue, *Hop.CA* group), a heatmap for controls, a heatmap for *Hop.CA* overexpression, gene names, and PCA analysis, are shown. According to transcriptome analysis of the tracheal epithelium 1128 genes ($p < 0.05$) were down-regulated, 876 genes ($p < 0.05$) were up-regulated. The changes in the gene expression total value were not significant in the ectopic expression trachea compared to the controls. (B) The inhibition of the JAK/STAT signaling by ectopic expressing *Dome.DN* for 18 hours affects the transcription of 814 genes, however, which only 102 genes were regulated in both types of airways; with ectopically activated and inhibited JAK/STAT signaling.

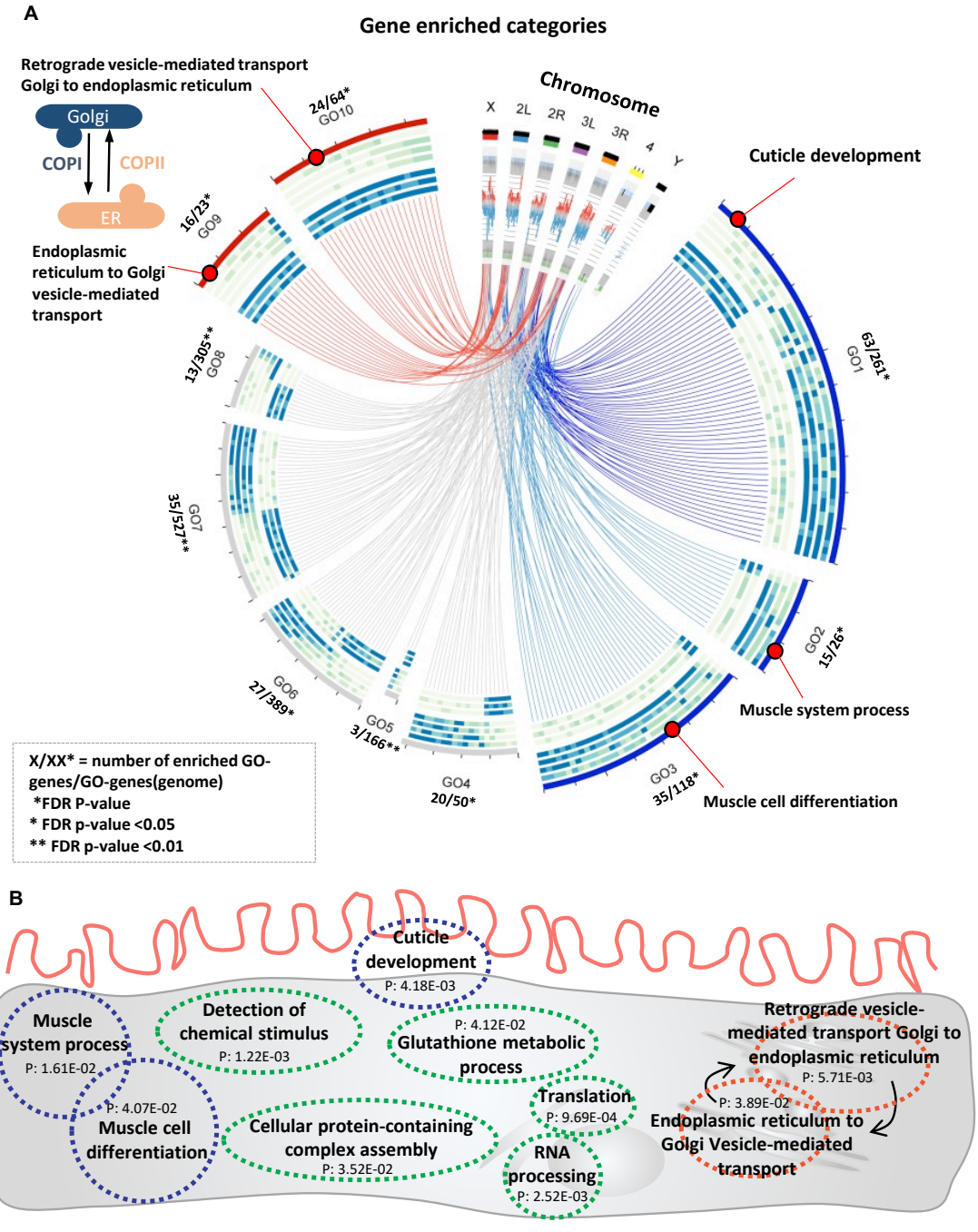

Figure 7: Gene Ontology (GO) enrichment analysis of the 2004 annotated differentially expressed genes in *Hop.CA* overexpressing airways vs controls. (A) Gene ontology analysis showed 10 biological processes that were enriched in *Hop.CA* overexpressing airways compared with matching controls. Most regulated genes in the GO1, GO2, and GO3 groups were down-regulated. Most regulated genes that involved in the COPI-and COPII-mediated vasicular transport between endoplasmic reticulum and Golgi (GO9 and GO10) were up-regulated. GO1, cuticle development; GO2, muscle system process; GO3, muscle cell differentiation; GO4, glutathione metabolic process; GO5, detection of chemical

766 stimulus; GO6, cellular protein-containing complex assembly; GO7, RNA processing; GO8, translation;
767 GO9, endoplasmic reticulum to Golgi vesicle-mediated transport; GO10, retrograde vesicle-mediated
768 transport Golgi to the endoplasmic reticulum. (B) Enriched biological processes were superimposed on
769 a sketch depicting a tracheal epithelial cell, with the corresponding *p*-value added. Blue indicates
770 processes where genes were mainly down-regulated; red indicates processes where genes were mainly
771 up-regulated; green indicates processes where genes were both down-regulated and up-regulated at
772 similar extents. See also table S10 for annotation of genes involved in each process. All processes
773 shown displayed $p < 0.05$ (Fisher's exact test).

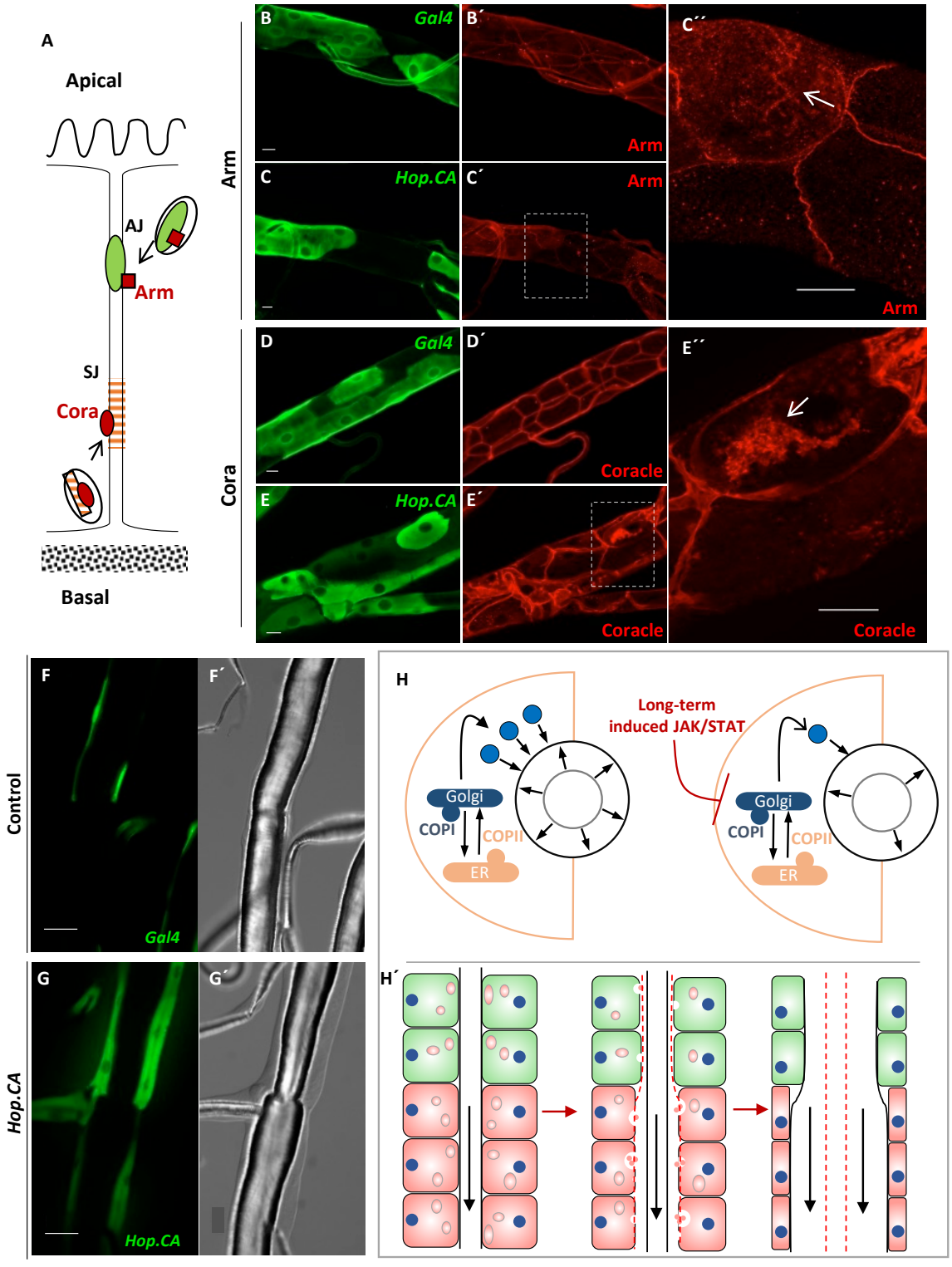

Figure 8: Activation of airway epithelial JAK/STAT signaling affects vesicle-mediated transport of proteins. (A-E) Coracle (Cora) and Armadillo (Arm) localization in airway epithelial cells. (A) shows the schematic orientation of Arm and Cora only at the contact zone between two airway epithelial cells.

Adherens junction (AJ), Septate junction (SJ). Trachea of *vvl-coin* larvae (control; B and D) and *vvl-coin>Hop.CA* larvae (treatment; C and E) stained for GFP (green, Gal4 positive cells), Arm or Cora (red), respectively. 30 specimens were investigated in each group. (F-G) Micrographs of the trachea of *vvl-coin* larvae (control; F) and *vvl-coin>Hop.CA* larvae (treatment; G). White are places where tracheal stenosis took place in the regions with cells expressing *Hop.CA* to a high degree. Scale bar: 20 µm in A-E; 50 µm in F-G. (H) Schematic illustration of the thickening of the epithelium and narrowing of the tube. In the control epithelium, a secretory burst of luminal proteins drives the diametric expansion of the tubes and this process depends on vesicle-mediated transport. COPI-and COPII-mediated vesicular transport plays a central role in this process, mutation members in the process underly the tube size defect in previous reports [27, 28]. However, long-term induced JAK/STAT activation impedes vesicle-mediated transport that can be reflected by the deregulation of massive genes involved in COPI-and COPII-mediated vesicular transport. This dysfunction of transport led to the appearance of tube size defect such as the increase in the cell volume and narrowing the tube size.

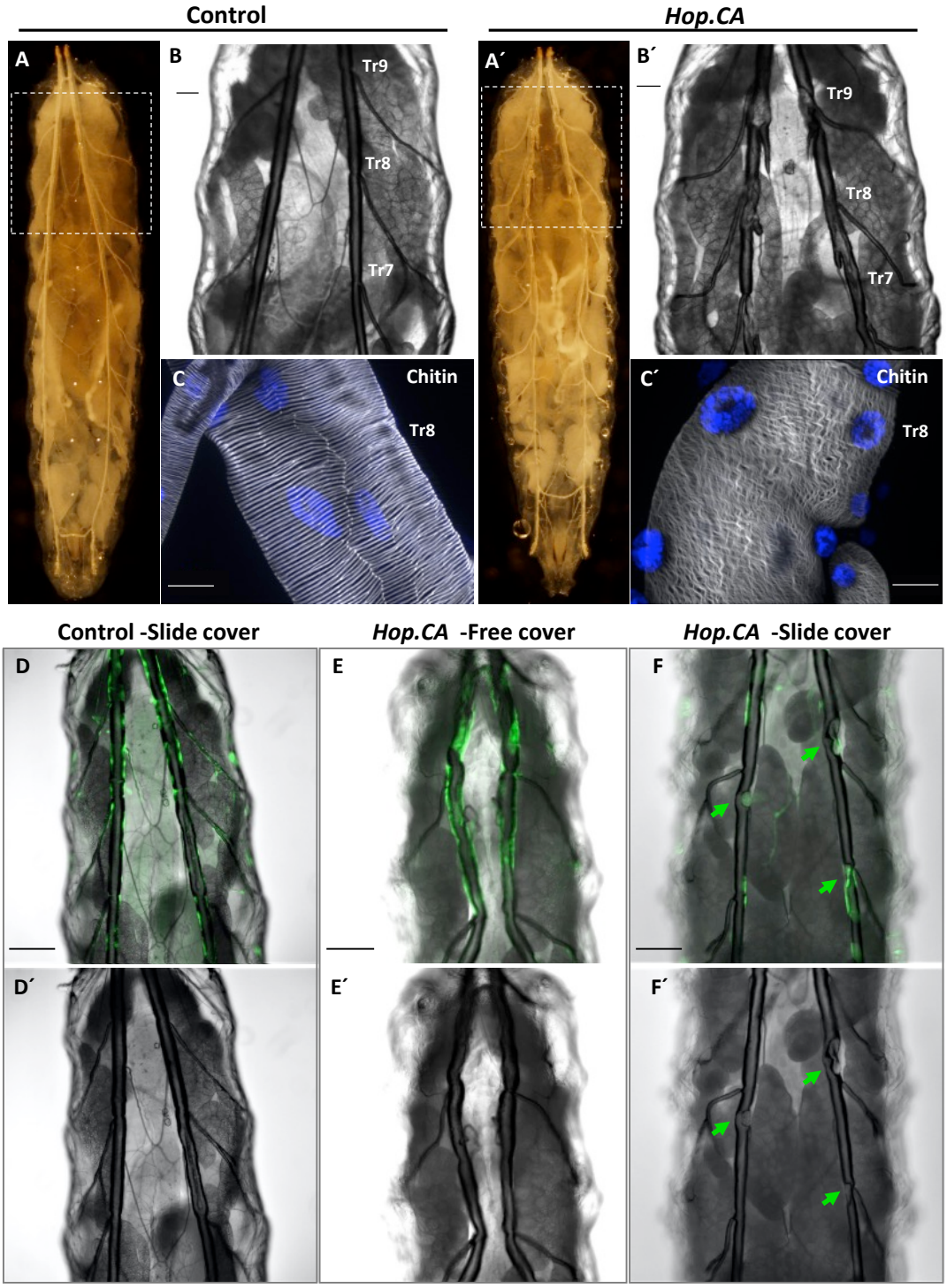

Figure 9: Activation of JAK/STAT signaling in airway epithelial cells affects the development of the epicuticle. (A-C) Activation of JAK/STAT signaling in airway epithelia observed in whole larvae by expressing *UAS-Hop.CA* under the control of the *btl.ts*. Controls (A-C) and induction of expression by shifting the temperature to 29 ℃ causes the defects in the tracheal epicuticle (A'-C'). 50 control larvae

797 and *btl.ts>Hop.CA* larvae were investigated in A-C. (A, A') Overview of the whole larvae showing the
798 whole tracheal system. In (B, B') the region containing Tr7-Tr9 is shown. (C, C') Chitin staining of isolated
799 airways (at the Tr8 region). (D-F) Micrographs of the trachea of *vvl-coin* larvae under different
800 conditions. In D, D' the control is shown, in E, E', the undisturbed larval of animals experiencing *Hop.CA*
801 overexpression are displayed. F, F' similar animals as in E, E', but the animals covered with a slide,
802 inducing a certain degree of compression. The arrows show the collapsed sites in the tracheal tube.
803 30 larvae in each group were investigated in D-F. Scale bar: 50 µm in B; 20 µm in C; 200 µm in D-F.

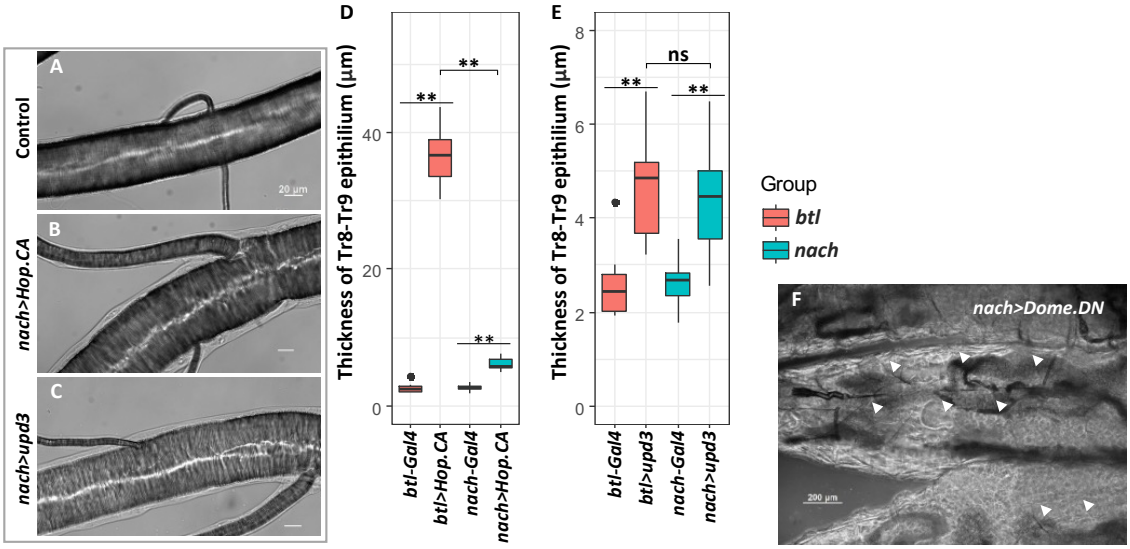

804

805 Figure 10: Mild activation of epithelial JAK/STAT signaling mitigated the thickening phenotype. (A-C)
806 Micrographs of the Tr8-Tr9 regions of *nach-Gal4* larvae (control, A), *nach>Hop.CA* (treatment, B), and
807 *nach>upd3* larvae (treatment, C). (D-E) Quantification of the epithelial thickness of the Tr8-Tr9 region
808 of those larvae whose JAK/STAT signaling were activated by expressing *Hop.CA* or *upd3* under the
809 control of *nach-Gal4* and *btl-Gal4*. (F) Micrographs of *nach>Dome.DN* larvae experiencing suppression
810 of the JAK/STAT pathway make trachea translucent and filled with fluids (arrows); triangle indicates the
811 tracheal position. 30 larvae in each group were used to quatify the thickness. ns means not significant,
812 * $p < 0.05$, ** $p < 0.01$ by Student's t-test. Scale bar: 20 µm in A-C; 200 µm in F.

813

814

815

816

817